

Rational synthesis of pindolol imprinted polymer by non-covalent protocol based on computational approach

Kiran Kumar Tadi · Ramani V. Motghare

Received: 26 December 2012 / Accepted: 16 April 2013 / Published online: 18 May 2013
© Springer-Verlag Berlin Heidelberg 2013

Abstract Pindolol (PDL) is a potent and specific adrenoreceptor blocking agent. It is widely used in the treatment of hypertension, cardiac arrhythmia and angina pectoris. Molecularly imprinted polymers (MIPs) are synthetic receptors having potential applications in drug delivery systems and devices such as diagnostic sensors. In the present work, *ab initio* quantum mechanical simulations and computational screening were used to identify functional monomer having best interactions with PDL. A virtual library of 16 functional monomers was built and the possible minimum energy conformation of the monomers and PDL were calculated using Hartree-Fock (HF) method for the synthesis of PDL imprinted polymer. The interaction energy between functional monomer and the template were corrected by means of basis set superposition error (BSSE) in all pre-polymerization complexes. The hydrogen bonding between PDL and functional monomer was evaluated by changes in bond lengths before and after complex formation. The virtual template-monomer complex with highest interaction energy is more stable during the polymerization and leads to high selectivity and specificity toward the template. The interaction energy of PDL was found to be the highest with itaconic acid followed by 4-vinyl pyridine and least with acrylonitrile. Taking a spectroscopic viewpoint, results obtained from analysis of the harmonic infrared spectrum were examined. Red and blue shifts related to the stretching frequencies of either donors or acceptors of protons were identified and compared experimentally. Stoichiometric mole ratio of template to functional

monomer was optimized and confirmed by UV visible spectra titrations. The theoretical results were correlated by evaluation of binding parameters of MIPs. The experimental binding results were in good agreement with theoretical computations.

Keywords BSSE · Computational approach · Hydrogen bonding · L-F isotherm · Molecularly imprinted polymers · Pindolol

Introduction

Molecular imprinting technique is used for the creation of selective recognition sites in synthetic polymers. The principle involved is similar to the “lock and key” system proposed by Fischer to describe the specificity of enzymes [1]. Molecularly imprinted polymers are obtained by thermal or UV irradiated co-polymerization of functional and cross-linking monomers in the presence of target analyte (template) of interest. Then the template molecule is extracted, forming cavities complementary to its shape and size of the template in polymer matrix [2]. The reference polymer or non-imprinted polymer (NIP) is also prepared as MIP but in the absence of template. The selectivity and robustness of imprinted polymers is provided by protecting the shape and size of cavities during the polymerization by using proper functional monomer and crosslinker. In the last two decades, molecular imprinting has become an important technique for assembling polymeric artificial receptors. MIPs become increasingly attractive in many fields of chemistry and biology, particularly as an affinity material for sensors [3–5] biomimetic assays [6], adsorbents for chromatographic stationary phases [7–9] and solid phase extraction [10, 11]. In spite of vast applications of MIPs, selection of suitable functional monomer and optimization

Electronic supplementary material The online version of this article (doi:10.1007/s00894-013-1856-2) contains supplementary material, which is available to authorized users.

K. K. Tadi · R. V. Motghare (✉)
Department of Chemistry, Visvesvaraya National Institute
of Technology, Nagpur 440011, India
e-mail: rkkawadkar@chm.vnit.ac.in

of template to functional monomer ratio makes imprinting protocol tedious and time consuming.

Combinatorial chemistry and molecular modeling are the two most promising tools for the development of MIPs with enhanced recognition properties [12]. Takeuchi *et al.* introduced combinatorial screening of functional monomer for ametryn imprinting with an automatic dispenser [13]. In general, standard formulations using chemical intuition can be exclusively found in literature. However, because of slow analysis methods, these procedures are time consuming and cannot be used for screening of a large library of compounds [14].

Screening for proper functional monomer can be carried out by exhaustive search *via* manual [15] or automatic [16] combinatorial approach. Although combinatorial methods are more rapid than traditional approach [17] they are expensive since many conditions would be evaluated. Computer aided study of MIP is a rational and fast method for searching optimal imprinting conditions in order to improve the recognition properties of MIP. Molecular mechanics (MM) and quantum mechanics (QM) are the two channels for modeling molecules. MM calculations have been used for computational screening of functional monomer against a molecular model of a template as a standard protocol for rational design of MIP [18–20]. The major advantage of MM methods are the capability of dealing with systems containing large number of atoms within a relatively short computing time [21] but in principle more reliable results can be obtained by using quantum mechanics.

Ab initio calculations based on quantum mechanics at different theory levels, such as HF [22–24], Moller-Plesser [25] or density functional theory [26] have been published to design MIPs. The *ab initio* calculations of intermolecular interactions result invariably in over estimation of the true value. The discrepancy arises from the phenomena known as basis set superposition error (BSSE). BSSE was first reported by Mukawa *et al.* for design of MIPs using computational approach and refers to the correction of this error [27]. By taking the article as first reference, the structures were optimized by HF method and energies were calculated by B3LYP/6-31+G(d,p) level theory corrected by means of BSSE. The HF level of theory was chosen instead of high level of theories with an aim of describing a system accurately at minimum computation time and cost. Selection of functional monomers for the synthesis of MIPs for β -blockers using molecular modeling and simulation method were not yet reported. Hattori *et al.* reported the use of molecular modeling to identify the binding sites of bopindolol and its two metabolites with beta 1-adrenoreceptors [28].

In this paper, the authors prepared a virtual library of 16 functional monomers for PDL using Gaussian03 software. PDL, a β -adrenoreceptor antagonist used in the treatment of hypertension, angina pectoris and other cardiovascular disorders [29]. The functional monomer that can form the most stable pre-polymerization complex with PDL was selected by computing interaction energy between functional monomers and the

template. The method followed in the present work shows a simple and elegant way to use computer simulation to reduce experimental time and cost especially when the template is expensive.

Materials and methods

Hardware and software

The personal computer used to simulate functional monomers was Intel Pentium 4 running with Red Hat Linux operating system, 2.0 GHz CPU, 2 GB RAM and 200 GB hard disc. This system was used to execute software package Gaussian 03. Avogadro 1.0.1 provided graphical user interface for Gaussian.

Geometry optimization and energy calculations

Computational designing of MIP was performed in several steps as follows.

Building of virtual library: In the first step, three-dimensional structures of the template, monomer and monomer-template complexes were built up with the aid of Avogadro program (<http://avogadro.openmolecules.net/>) and pre-optimized by MMFF [30] force field applying its implementation in the Avogadro program [31]. The virtual library of functional monomers consists of acidic, basic and neutral monomers.

The Cartesian co-ordinates of stable conformers generated in Avogadro were used to prepare input file for running the Gaussian simulations. The molecular geometries were optimized by using Hartree-Fock method with 6-31G(d) basis set implemented in Gaussian 03 [32]. The optimizations were followed by computations of the harmonic vibrational frequencies to check local minima and no imaginary frequencies were obtained.

Interaction energy calculations: The single point energy of each optimized conformation was computed by using B3LYP/6-31+G(d,p) basis set. The interaction energy (ΔE) of pre-polymerization complexes were calculated by using Eq. 1

$$\Delta E = E(\text{template} - \text{monomer}) - E(\text{template}) - \sum E(\text{monomer}) \quad (1)$$

where $E(\text{template-monomer})$ is the energy of template-monomer complex, $E(\text{template})$ is the energy of PDL and $E(\text{monomer})$ is the energy of the monomer. The basis set superposition error (BSSE) which often substantially affects the calculated stabilization energies, was corrected by means of the counterpoise method [33].

Experimental methods

Pindolol (PDL), itaconic acid (IA) and acrylonitrile (AN) were purchased from Sigma-Aldrich. Ethylene glycol dimethacrylate (EDGMA) and acetonitrile HPLC grade from Merck. 4-Vinylpyridine (4-VP) and 2, 2'-Azobisisobutyronitrile (AIBN) were supplied by Across organics. AIBN was recrystallized from methanol before use. All chemicals were of analytical grade unless mentioned and all aqueous solutions were prepared in MilliQ water. Standard sieve of BSS number 200 was used to get fine particles.

A Shimadzu model UV-1800 spectrophotometer equipped with quartz cell of 1 cm path length was used for recording absorbance spectra. The FTIR spectra of the PDL imprinted polymers were recorded *via* Shimadzu model IRAffinity FTIR spectrometer using KBr pellet method. Toshniwal pH meter was used for measuring pH.

Preparation of PDL imprinted and non-imprinted polymers

The PDL imprinted polymers were prepared by bulk polymerization imprinting technique with molar ratio of template: monomer: crosslinker as 1:2:40. Three sets of MIP/non-imprinted congener (NIPs) pairs were prepared by mixing 0.25 mmol of PDL (template), 0.50 mmol of functional monomer (IA, 4-VP or AN) and 5 ml of acetonitrile in 15 ml glass vial. The contents were shaken well to allow for self assembly of the host-guest complexes. Subsequently, 10 mmol of EDGMA (crosslinker) and 0.15 mmol of AIBN (initiator) were added. The mixture was purged with nitrogen for 10 min to create inert atmosphere. The vial was completely sealed and kept in water bath at 55 °C for 12 h to complete polymerization reaction. The resultant monoliths were obtained by breaking the glass vials. The control or non-imprinted polymer was also prepared in the same manner but in absence of PDL. NIPs were washed with methanol to remove the un-reacted precursors. The polymers were ground by using mortar and pestle and sieved with a standard sieve of size 75 μm to get fine particles.

The imprinted polymers (MIPs) were repeatedly washed with methanol/acetic acid (10:1 v/v) to extract the template and complete elution of template was confirmed from disappearance of the absorption peak at 263 nm in UV spectra [34]. The particles were washed with 1 mmol L⁻¹ Na₂CO₃ solution followed by water to remove the residual acetic acid, dried under vacuum at 50 °C overnight and then used for further studies.

UV-visible titration studies

Pre-polymerization complexes of different template to monomer ratio in acetonitrile varying from 1:1 to 1:4 were prepared as follows. Fixed quantity of PDL (0.1 mmol L⁻¹) were added to monomers (IA, 4-VP and AN) of different concentrations

viz., 0.1 mmol L⁻¹, 0.2 mmol L⁻¹, 0.3 mmol L⁻¹, 0.4 mmol L⁻¹ in acetonitrile. The UV absorbance spectra of the pre-polymerization complexes were recorded.

Effect of medium pH on adsorption

Adsorption studies were performed at different pH media (2–9) to investigate the optimum pH, at which PDL adsorbs maximum amount onto the imprinted polymer. Fifty mg of MIP_{IA} was added to 20 ml of 60 $\mu\text{g/ml}$ PDL solution and the mixture was shaken for 4 h. Then the samples were centrifuged and the free PDL was determined.

Batch rebinding studies

The binding capacity of MIP and NIP were determined by batch rebinding experiments. In the binding assay, 50 mg of MIP or NIP was added to 20 ml of the PDL solution of different concentrations (5–90 $\mu\text{g/ml}$) in phosphate buffer (optimum pH=6) and stirred for 4 h at 25 °C. The polymer particles were filtered off and the filtrate was analyzed for PDL by UV/VIS spectrophotometer at an absorption wavelength of 263 nm. The quantity of the bound analyte was determined by subtracting equilibrium quantity of the template from initial amount of the template. The binding experiments were carried out twice for each adsorbent. The experimental binding data were fitted to the Langmuir-Freundlich adsorption model.

Results and discussion

Selection of functional monomer for synthesis of PDL imprinted polymer

The interaction energy between PDL and each functional monomer (Table 1) selected from the virtual library was investigated to screen the most suitable functional monomer. The computer simulation experiment identified IA and 4-VP as the most promising monomers capable of forming stronger interactions with the template. The interesting and noticeable thing is that 4-VP which has only one hydrogen bond acceptor has been found to be best functional monomer after IA. This may be due to the secondary electrostatic and polarization interactions of polar functional groups located close to hydrogen bonding sites significantly stabilizing the H-bonding interactions [35]. The optimized conformations of PDL and three functional monomers are shown in Fig. 1.

Functional monomers *viz.*, vinyl imidazole, 2-hydroxy ethyl methacrylate, p-vinyl benzoic acid and *trans*-(3-pyridyl)-acrylic acid has moderate interaction energy while AN has

Table 1 Interaction energies of pre-polymer complexes between pindolol and functional monomers

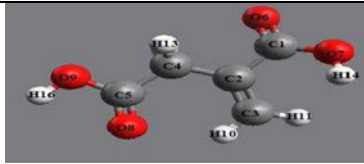
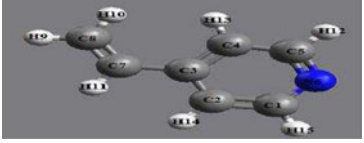
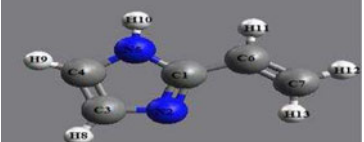
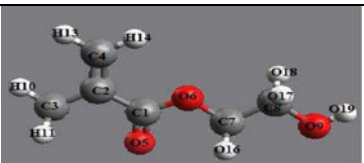
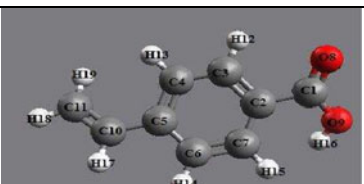
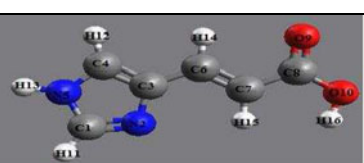
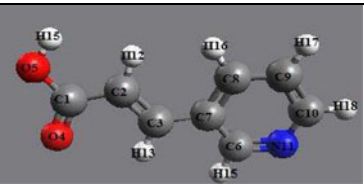
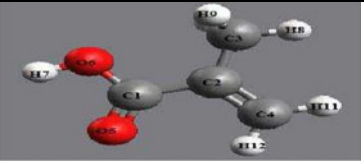
Functional monomer	Optimized Structure	Nature of functional monomer	Interaction energy ΔE (kcal/mol)
Itaconic acid		Acidic	-16.8486
4-Vinylpyridine		Basic	-12.0545
Vinylimidazole		Amphoteric	-11.2701
2-Hydroxyethyl methacrylate		Neutral	-10.1719
p-Vinyl benzoic acid		Acidic	-9.8446
Uraconic acid		Acidic	-9.8205
Trans-3-(3-pyridyl)-acrylic acid		Neutral	-9.7954
Methacrylic acid		Acidic	-6.9264

Table 1 (continued)

Functional monomer	Optimized Structure	Nature of functional monomer	Interaction energy ΔE (kcal/mol)
2-(Trifluoromethyl) acrylic acid		Acidic	-5.9613
Acrylamide		Neutral	-5.6978
Acrylic acid		Acidic	-5.3338
N,N'-Diethyl-4-styrylamidine		Basic	-2.9869
N,N'-Methylene bisacrylamide		Neutral	-2.6412
N-(4-Vinylbenzyl)iminodi acetic acid		Acidic	-1.6999
Acrylamido-2-methyl-1-propane sulfonic acid		Acidic	-1.20482
Acrylonitrile		Neutral	-0.5522

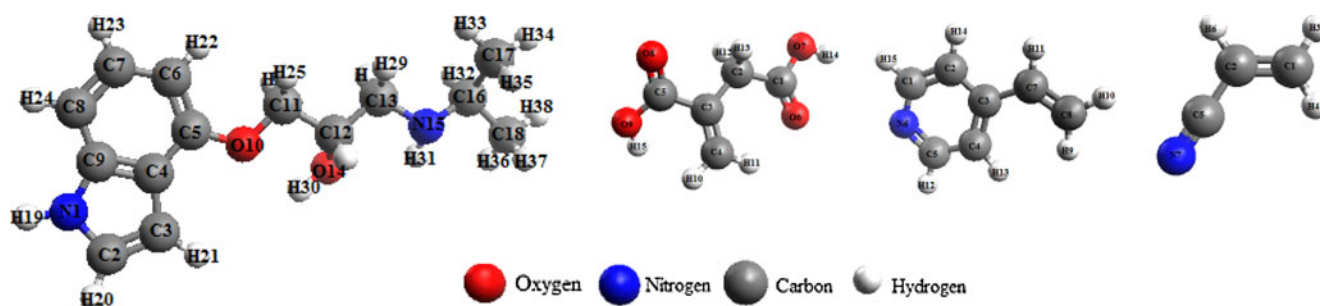


Fig. 1 Optimized conformations of PDL, IA, 4-VP and AN

been found to have the weakest interactions with PDL. Further computational study was focused on the complexes with the highest, moderate and the lowest energies. The energies of the complexes and the corresponding values for BSSE correction are given in electronic supplementary material (Table S1).

Nature of PDL and functional monomer intermolecular interactions

Template monomer complexes having the highest, moderate and the lowest interaction energy were analyzed further to

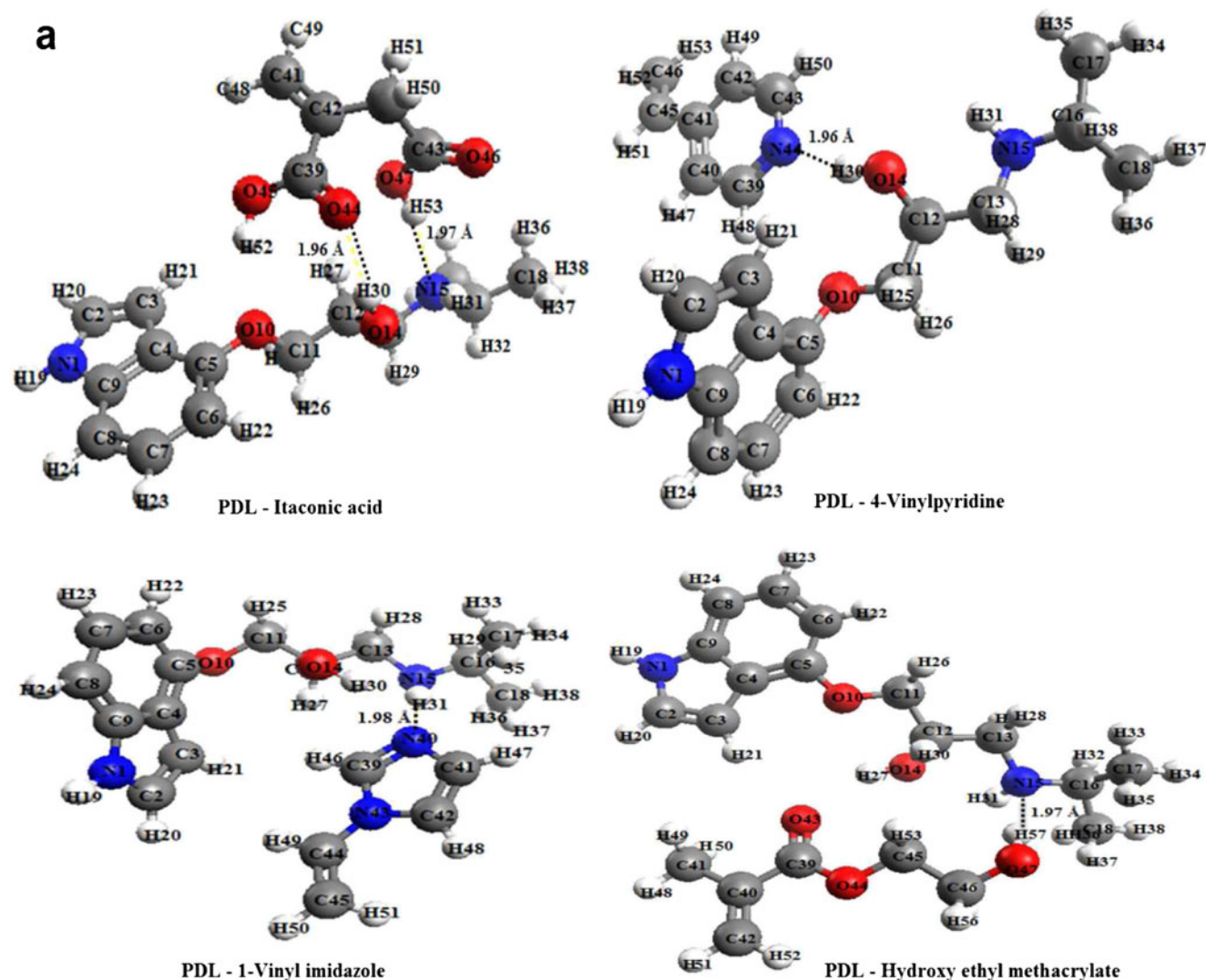


Fig. 2 a Optimized structures of prepolymerization complexes of pindolol with functional monomers, b Optimized structures of prepolymerization complexes of pindolol with functional monomers

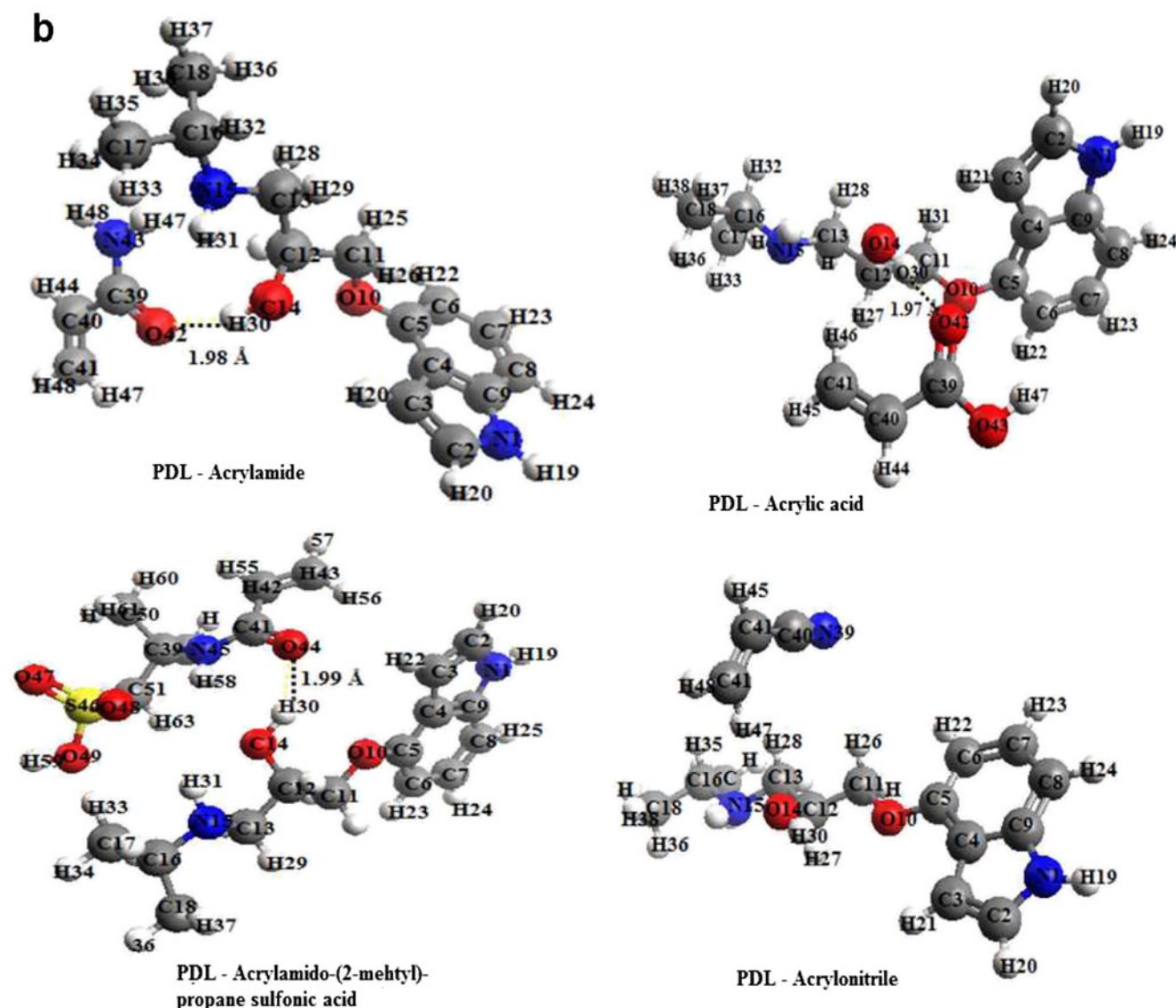


Fig. 2 (continued)

determine and characterize interactions between PDL-functional monomer complexes. The optimized structures of pre-polymerization complexes are shown in Fig. 2a and b. The design and successful imprints require basic understanding of the fundamental forces that lead to self-assembly of template-monomer complex and the rebinding of ligands to the final MIP [36]. It is clear from the interaction energy of the functional monomers, IA was found to be the most suitable functional monomer for synthesis of PDL imprinted polymer. Increase in the interactions between template and functional monomer can enhance overall binding affinity as well as the substrate specificity [37]. Unlike all other functional monomers, IA interacts with PDL *via* two hydrogen bonds. In the pre-polymer complex, one -C=O groups of carboxylic acid acts as a H-bond acceptor and the -O-H group of another carboxylic group acts as H-bond donor.

This is in good agreement with the fact that the more number of interactions, the more stabilized the pre-polymerization complex and hence higher interaction energy.

The strongest hydrogen bond in the most stable PDL-IA (1:1) complex is the bond between O-H group of PDL and carbonyl group of IA with bond distance 1.96 Å. This interaction enhanced by the presence of another hydrogen bond formed between amino group of PDL and hydroxyl group of IA with bond distance 1.97 Å. The hydrogen bond distance shows the highest possible hydrogen bonding between PDL and IA. These bond distances are less in comparison to reports for harmine [8] and benzo(α) pyrene [25] imprinting.

Even though 4-VP forms one hydrogen bond with PDL, it may have been stabilized by electrostatic contribution of pyridine ring [35]. Weaker interactions were found between PDL and functional monomers N,N'-diethyl-4-styryldiamine, N,N'-

methylene bisacrylamide, N-(4-vinylbenzyl) iminodiacetic acid, acrylamido-(2-methyl)-propane sulfonic acid and acrylonitrile.

Variation in bond length

The whole hydrogen bonding data of precursors and series of optimized complexes are represented in Table 2, where the D, H and A introduce the donor, bridging hydrogen and acceptor atoms respectively.

Hydrogen bonding between template and functional monomer plays a vital role in stabilizing the pre-polymerization complex as compared to ionic bonds, dipole-dipole and electrostatic interactions. Hence to find extent of hydrogen bonding, change in bond length (Δd) before and after complex formation between PDL and functional monomer were studied. Inspection of geometries of pre-polymerization complex reveals that there is a significant change in bond lengths in hydroxyl (O-H) and amino (N-H) groups of PDL and functional monomer groups. It is clear from Table 2, for PDL-IA complex the change in bond lengths were 0.024 Å and 0.013 Å

(O-H₃₀···₄₄O = C), 0.015 Å and 0.017 Å (H-N₁₅···₅₃H-O) bonds.

Variation in IR vibrational frequencies

A vibrational analysis of all template-monomer complexes was carried out to examine the main alternations in vibration modes of proton donors and acceptors (red or blue shift). According to the values summarized in Table 3, PDL-IA complex exhibits red shift in the O-H bond and a slight blue shift in N-H bond. On the other hand, PDL-VIM complex exhibits red shift in the N-H bond because the amino group of PDL is acting as a proton donor [38]. It is very interesting that in PDL-AN complex no blue or red shifts were observed. This is in accordance with the lower interaction energies and no change in bond lengths after complex formation for this complex. In this way, a clear red shift in proton donors and a slight blue shift in proton acceptors were observed in all complexes (except PDL-AN). The experimental FTIR spectra of the synthesized MIPs without

Table 2 Change in the bond lengths of the groups due to the complex formation

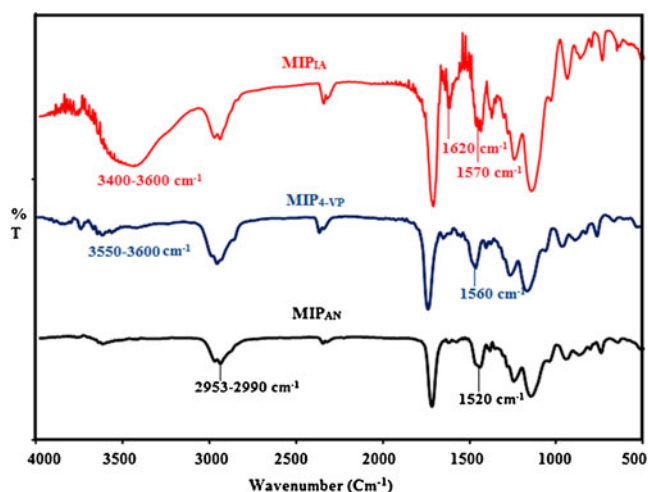
Template-monomer complex	D–H···A	d_{initial} (H···A)	d_{complex} (H···A)	Δd (Å) ($d_{\text{complex}} - d_{\text{initial}}$)
PDL-Itaconic acid	i) d(O-H ₃₀ ···O ₄₄ = C)			
	d(O-H ₃₀)	0.948	0.972	0.024
	d(O = C ₄₄)	1.184	1.197	0.013
	ii) d(H-N ₁₅ ···H ₅₃ -O)			
	d(H-N)	1.001	1.016	0.015
PDL-4-Vinylpyridine	d(O-H)	0.953	0.970	0.017
	d(O-H ₄₉ ···N ₃₆ = C)			
	d(O-H ₄₉)	0.948	0.959	0.011
PDL-Vinylimidazole	d(N ₃₆ = C)	1.318	1.334	0.016
	d(N-H ₃₁ ···N ₄₀ = C)			
	d(N-H ₃₁)	1.001	1.026	0.025
PDL-Hydroxyethyl methacrylate	d(N ₄₀ = C)	1.296	1.316	0.020
	d(H-N ₁₅ ···H ₅₇ -O)			
	d(H-N ₁₅)	1.001	1.010	0.009
PDL-Acrylamide	d(H ₅₇ -O)	0.942	0.956	0.014
	d(O-H ₃₀ ···O ₄₂ = C)			
	d(O-H ₃₀)	0.948	0.954	0.006
PDL-Acrylic acid	d(O ₄₂ = C)	1.20	1.210	0.014
	d(O-H ₃₀ ···O ₄₂ = C)			
	d(O-H ₃₀)	0.948	0.963	0.015
PDL-Acrylamido-2-methyl)-propane sulfonic acid	d(O ₄₂ = C)	1.190	1.220	0.010
	d(O-H ₃₀ ···O ₄₄ = C)			
	d(O-H ₃₀)	0.948	0.955	0.007
PDL-Acrylonitrile	d(O ₄₄ = C)	1.222	1.210	0.012
	No H-bond			
	d(O-H)	0.948	0.948	No Change
	d(N-H)	1.001	1.001	
	d(N \equiv C)	1.137	1.137	

Table 3 Values of the stretch frequencies (cm^{-1}) for template and functional monomers before and after complex formation

Molecule/complex	Modes				
	N-H _{Stretch}	N-H _{Bend}	O-H	C = O	C = N
Pindolol	3297	1520	3379	–	–
Itaconic acid(IA)	–	–	3351	1605	–
PDL-Itaconic acid (O-H \cdots O = C and H-N \cdots H-O)	3298	1566	3363	1607	–
4-Vinylpyridine(4VPD)	–	–	–	–	1570
PDL-4VPD (O-H \cdots N = C)	–	–	3356	–	1602
1-Vinyl imidazole(VIM)	–	1497	–	–	1622
PDL-VIM (N-H \cdots N = C)	3216	–	–	–	1644
Hydroxyethyl methacrylate(HEMA)	–	1526	4192	–	–
PDL-HEMA(H-N \cdots H-O)	3310	–	4062	–	–
Acrylamide(ACR)	–	–	–	–	–
PDL-ACR(O-H \cdots O = C)	–	–	3363	1798	–
Acrylic acid (AA)	–	–	–	1810	–
PDL-AA (O-H \cdots O = C)	–	–	3285	1588	–
Acrylamido-2-methyl)-propane sulfonic acid(AMPSA)	–	–	–	1590	–
PDL-AMPSA (O-H \cdots O = C)	–	–	3296	1700	–
Acrylonitrile	–	–	–	1703	2607 ^a
PDL-AN	3295	1520	3379	–	2605 ^a

^a C \equiv N

extracting PDL are in shown in Fig. 3. A broad band in the spectrum of MIP_{IA} at 3400–3600 cm^{-1} shows the intra H-bonding between O-H and N-H moieties of IA and PDL complex. This band intensity decreased in MIP_{4-VP} spectrum due to formation of H-bond between N-H group of PDL and C = N group of 4-VP and finally diminished in MIP_{AN} spectrum due to the absence of H-bonding between AN and PDL. In the MIP_{IA} spectra, the bands at 1570 cm^{-1} and 1620 cm^{-1} correspond to N-H bending and C=O

**Fig. 3** Experimental FTIR spectra of molecularly imprinted polymers prepared with IA, 4-VP and AN

stretching respectively. In the case of MIP_{AN} spectrum, there are no shifts from their original position of bands. Thus, the experimental spectrum is in accordance with the theoretical vibrational frequencies of the complexes.

Optimization of template-monomer ratio

For a successful imprinting, it is important to optimize the ratio between number of moles of functional monomer and template. If excess moles of functional monomer are used, only a specific number of moles would react with template and the rest which remain in excess lead to non-specific binding [37], thus decreasing the binding capacity. So, the number of moles of functional monomer that interact with one mole of template was optimized. To reduce cost and computation time, optimization of template-monomer mole ratio was carried out on the selected functional monomers [25, 26]. The interaction energies of a stable complex of PDL with functional monomers in the ratios 1:1 to 1:4 were calculated for optimized conformations of these complexes (Table 4).

It can be seen from Table 4 that the interaction energies of template-monomer complexes increases up to a ratio of 1:2 and further increase in monomer ratio showed a downward trend. This shows the saturation of pre-polymerization complex at 1:2 template-monomer ratio. Therefore syntheses of all MIPs were carried out with 1 mol of PDL and 2 mol of functional monomer.

Table 4 Interaction energies of pre-polymerization complexes varying with monomer ratio

Template to FM ratio	$\Delta E(\text{kcal mol}^{-1})$		
	PDL-IA	PDL-4VP	PDL-AN
1:1	-16.849	-12.05	-0.552
1:2	-23.788	-15.395	-1.587
1:3	-19.874	-10.689	-1.016
1:4	-16.584	-4.806	-0.437

Stoichiometric analysis of template-monomer ratio

The pre-polymerization complex of PDL with three monomers (IA, 4-VP and AN) were examined by Job's method. This is a well known method often used to determine the stoichiometry of many kinds of complexes and is based on the spectral changes observed either for the host or the guest molecule [39–41]. The absorbance of solutions with different template to functional monomer ratio was measured and plotted as a function of molar fraction ($f_m = [M]/([T]+[M])$) to establish the Job's plot. The stoichiometry of pre-polymerization complex can be determined from the Job's plot according to the following Eq. 3,

$$n = \frac{f_{peak}}{(1 - f_{peak})} \quad (3)$$

where n is the stoichiometric ratio of pre-polymerization complex and f_{peak} is the molar fraction (f_m) corresponding to peak maxima in the Job's plot.

From Fig. 4a, it is clear that the peak maxima (f_{peak}) for IA and 4-VP were found at 0.66 indicates 1:2 stoichiometric ratio of the pre-polymerization complex. However, in the

case of AN (Fig. 4b) the absorbance increases gradually with the ratio but no peak was formed. This might have been due to the increase in concentration of functional monomer but no complex formation between AN and PDL. This was also confirmed by the theoretical hydrogen bonding and IR spectra analysis. (UV absorbance spectra are provided in supplementary material Fig. S1).

Analysis of rebinding capacity

The presence of acidic or basic medium affects the protonation equilibrium of secondary amine moiety of PDL and the carboxylic moiety of the MIP, with a strong impact on the hydrogen bond formation. The imprinted polymer MIP_{IA} showed higher affinity at pH value of 6, while in more acidic medium a gradual decrease in binding capacity was observed (electronic supplementary material Fig. S2). This result was in accordance with previous literature [42] showing acidic media caused decrease of the affinity of propranolol to the imprinted polymer. Moreover, since the pKa value of PDL is 9.16 [43] the slight acidic conditions provide good solubility of PDL. So the pH value of 6 was decided as optimum for batch rebinding studies.

The rebinding capacities of the three sets of MIPs prepared were evaluated by batch rebinding experiments. The experimental results reveal the proportionality between the theoretical interaction energy of the complexes and binding capacity of polymer. Binding capacity of MIPs prepared with functional monomer having the highest, next to the highest and the least interaction energies *viz.* IA, 4-VP and AN were studied by Langmuir-Freundlich (L-F) isotherm.

Although most of the imprinted polymers are modeled by using solely Freundlich or Langmuir isotherms, they cannot be used in both saturation and sub-saturation regions. The Langmuir isotherm best models the saturation behavior of MIP usually in the high concentration region, where as

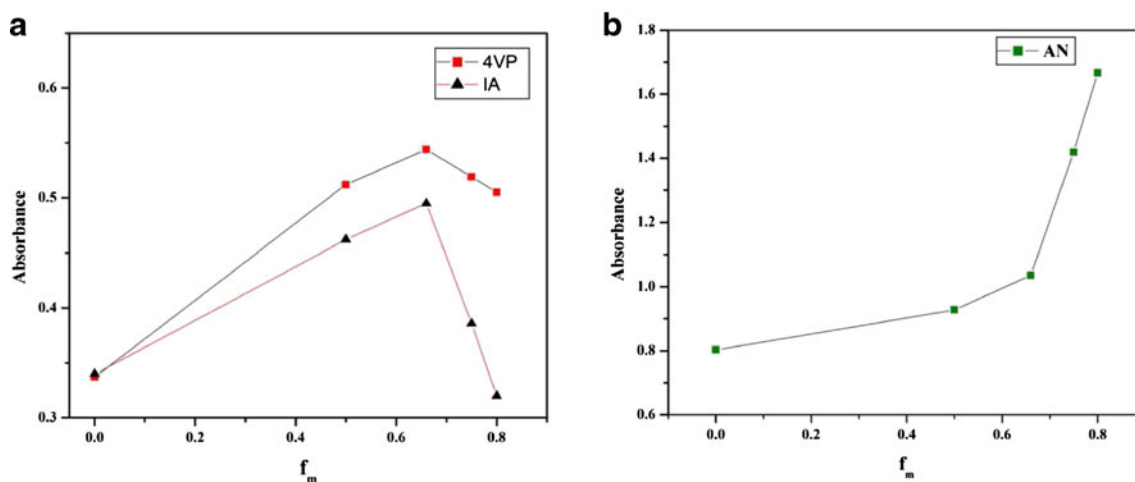
**Fig. 4** Job's plot presenting the relation between absorbance and molar ratio of template to functional monomer

Table 5 Langmuir-Freundlich fitting coefficients for the imprinted and non-imprinted congeners

Polymer	Fitting parameter			
	N_t ($\mu\text{mol g}^{-1}$)	a ($\text{g } \mu\text{mol}^{-1}$)	m	R^2
MIP _{IA}	125.76	0.0725	0.7355	0.9950
NIP _{IA}	73.86	0.0144	0.9765	0.9670
MIP _{4VP}	79.93	0.0594	0.8765	0.9860
NIP _{4VP}	60.95	0.0189	1.0913	0.9560
MIP _{AN}	56.732	0.0479	0.8798	0.9650
NIP _{AN}	37.86	$1.04 \cdot 10^{-3}$	0.9895	0.9660

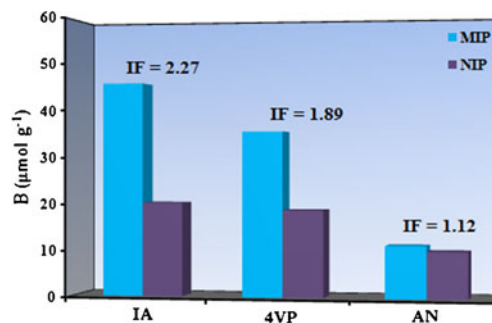
Freundlich is limited to the lower sub-saturation region of the binding isotherms. Langmuir-Freundlich model overcomes the limitation, which is uniquely suited to fit isotherms that have been measured over wide concentration regimes. The L-F isotherm model describes an equilibrium relationship between the amount of bound (B) and the amount of free analyte (F) such that:

$$B = \frac{N_t a F^m}{1 + a F^m} \quad (4)$$

where N_t is the total number of binding sites, B ($\mu\text{mol g}^{-1}$) is the amount of adsorbed analyte per unit weight of adsorbent, the variable 'a' is related to median affinity K ($K = a^{1/m}$) and 'm' is the heterogeneity index. It is clear from Eq. 4, when $m=1$ the equation reduces to Langmuir isotherm (homogeneous system) and when 'F' or 'a' approaches to '0' reduces to Freundlich isotherm (heterogeneous system). Equation 4 was used to fit the adsorption isotherm by a non-linear least square fitting to yield fitting parameters ' N_t ', 'a' and 'm' (Table 5).

It is evident from Table 5, MIP_{IA} have the highest number of binding sites and MIP_{AN} have the least number of binding sites. This is analogous to the binding energy values of PDL-IA and PDL-AN complexes. Moreover, all imprinted polymers show higher number of binding sites and higher affinity constant ($K = a^{1/m}$) than the corresponding NIPs. This shows the formation of binding pockets of specific shape and size of the template during the polymerization.

The descending order of binding sites (N_t) from MIP_{IA} to MIP_{AN} gives a clear proportional relation between the experimental and theoretical predictions. The formation of different kinds of binding sites during the polymerization can be a factor behind the higher heterogeneity index 'm' for all MIPs. As NIPs were prepared without addition of template (PDL), there was no scope for the formation of binding sites and hence the adsorption is only because of non-specific interactions with functional groups in the polymer.

**Fig. 5** Imprinting factors ($B_{\text{MIP}}/B_{\text{NIP}}$) of the polymers synthesized with different functional monomers

Imprinting effect of MIPs

The imprinting factor of the MIPs were determined at 60 $\mu\text{g/ml}$ concentration (i.e., at saturation) of PDL from the ratio of PDL bound to MIP (B_{MIP}) to that of corresponding NIP (B_{MIP}). With MIP_{IA} the ratio was found to be 2.2, while 1.89 for MIP_{4VP} and the least 1.12 found for MIP_{AN} (Fig. 5). This shows that the best binding interactions exist between IA and PDL in pre-polymerization complex, which are responsible for the formation of specific cavities in the polymer.

Conclusions

Rational synthesis of PDL imprinted polymer by non-covalent protocol was developed based on computational approach. A virtual library of 16 functional monomers was established to choose the functional monomer showing stronger interactions with PDL for the imprinted polymer synthesis. Computational calculations based on Hartree-Fock method was reincarnated by taking BSSE into consideration. The highest interaction energy was found for IA. Hydrogen bond formed between PDL and functional monomer, was characterized by changes in bond lengths and IR vibrational frequencies after complex formation. The theoretical predictions were proved by adsorption capacity of the MIPs determined from batch rebinding experiments. The method describes not only selection of functional monomer for synthesis of MIP with optimal performance but also theoretical characterization in a simple and elegant way. Selection of functional monomer for the synthesis of MIP by computational approach effectively reduces time and wastage of chemicals especially for PDL like expensive templates.

Acknowledgments We are Grateful to Electronics and Communication Engineering Department, Visvesvaraya National Institute of Technology, Nagpur for giving opportunity to work on Gaussian Software.

References

1. Fischer E (1894) *Ber Dtsch Chem Ges* 27:2985–2993
2. Garcia-Calzon JA, Diaz-Garcia ME (2007) *Sensor Actuat B Chem* 123:1180–1194
3. Dickert FL, Lieberzeit P, Tortschanoff M (2000) *Sensor Actuat B Chem* 65:186–189
4. Haupt K, Mosbach K (2000) *Chem Rev* 100:2495–2504
5. Kriz D, Ramstrom O, Mosbach K (1997) *Anal Chem* 69:345A–349A
6. Andersson LI (1996) *Anal Chem* 68:111–117
7. Bazylak G, Nagels LJ (2003) *IL Farmaco* 58:591–603
8. Hwang C-C, Lee W-C (2001) *J Chrom B* 765:45–53
9. Xie J, Zhu L, Luo H, Zhou L, Li C, Xu X (2001) *J Chrom A* 934:1–11
10. Hu X, Pan J, Hu Y, Li G (2009) *J Chrom A* 1216:190–197
11. Martin PD, Jones GR, Stringer F, Wilson ID (2004) *J Pharmaceut Biomed Anal* 35:1231–1239
12. Van Nostrum CF (2005) *Drug Discov Today* 2:119–124
13. Takeuchi T, Fukuma D, Matsui J (1998) *Anal Chem* 71:285–290
14. Karim K, Breton F, Roullin R, Piletaska EV, Guerreiro A, Chianella I, Piletsky SA (2005) *Adv Drug Deliv Rev* 57:1795–1808
15. Lanza F, Sellergren B (1999) *Anal Chem* 71:2092–2096
16. Lanza F, Hall AJ, Sellergren B, Bereczki A, Horvai G, Bayouhd S, Cormack PAG, Sherrington DC (2001) *Anal Chim Acta* 435:91–106
17. Batra D, Shea KJ (2003) *Curr Opin Chem Biol* 7(3):434–442
18. Chianella I, Lotierzo M, Piletsky SA, Tothill IE, Chen B, Karim K, Turner APF (2002) *Anal Chem* 74(6):1288–1293
19. Piletsky SA, Piletska EV, Karim K, Foster G, Legge C, Turner APF (2001) *Anal Chim Acta* 504:123–130
20. Subrahmanyam S, Piletsky SA, Piletska EV, Chen B, Karim K, Turner APF (2001) *Biosens Bioelectron* 16:631–637
21. Leach AR (2001) *Molecular modelling: principles and applications*. Prentice-Hall, Essex
22. Azenha M, Kathirvel P, Nogueira P, Fernando-Silva A (2008) *Biosens Bioelectron* 23(12):1843–1849
23. Riahi S, Ganjali MR, Moghaddam A, Norouzi P (2008) *J Mol Model* 14:325–333
24. Liqing W, Sun B, Li Y, Chang W (2003) *Analyst* 128:944–949
25. Khan M, Wate P, Krupadam RJ (2012) *J Mol Model* 18:1969–1981
26. Liu R, Li X, Li Y, Jin P, Qin W, Qi J (2009) *Biosens Bioelectron* 25:629–634
27. Mukawa T, Goto T, Nariai H, Aoki Y, Imamura A, Takeuchi T (2003) *J Pharmaceut Biomed Anal* 30:1943–1947
28. Nakaruma I, Suzuki A, Ohnuki T, Hattori K, Watanabe K, Kurose H, Nagao T, Nagatomo T (2000) *Pharmacology* 61:6–10
29. Jack DB (1992) *Handbook of clinical pharmacokinetic data*. Macmillan, London
30. Halgren TA (1996) *J Comput Chem* 17:490–519
31. Roberta DS, Mario RL, Mario A, Fabio DS, Donato C, Giuseppe V (2009) *Molecules* 14:2632–2649
32. Gaussian 03 (2004) R.C., Gaussian, Inc. Wallingford, CT, USA
33. Boys SF, Bernardi F (1970) *Mol Phys* 19:553–566
34. Panderi I, Parissi-Poulou M (1994) *J Pharm Biomed Anal* 12:151–156
35. Uchimaru T, Korchowec J, Tsuzuki S, Matsumura K, Kawahara S (2000) *Chem Phys Lett* 318:203–209
36. Yan M, Ramstrom O (2005) *Molecularly imprinted materials*. Marcel Dekker
37. Komiyama M, Takeuchi T, Mukawa T, Asanuma H (2003) *Molecular Imprinting: From Fundmentalls to Applications*. WILEY-VCH
38. Oliveira BZ, Araujo Regiane CMU (2012) *J Mol Model* 18:2845–2854
39. Laudy D, Tetrat F, Traunt E, Blach P, Furnmentin S, Surpateanu G (2007) *J Incl Phenom Macrocyll Chem* 57:409–413
40. Striegler S, Ditte M (2003) *Anal Chim Acta* 484:53–62
41. Svenson J, Karlsson JG, Nicholls IA (2004) *J Chrom A* 1024:39–44
42. Demirel M, Sevin SB, Say R, Yazan Y (2007) *FABAD J Pharm Sci* 32:147–157
43. Babic S, Alka JMH, Dragana Mutavdzic P, Marija KM (2007) *Trends Anal Chem* 26:1043–1061